Elastic differential cross sections for C4F6 isomers in the 1.5–200 eV energy electron impact: Similarities with six fluorine containing molecules and evidence of F-atom like scattering

M. Hoshino, P. Limão-Vieira, K. Anzai, H. Kato, H. Cho, D. Mogi, T. Tanioka, F. Ferreira da Silva, D. Almeida, F. Blanco, G. García, O. Ingólfsson, and H. Tanaka

Citation: The Journal of Chemical Physics **141**, 124302 (2014); doi: 10.1063/1.4895903
View online: http://dx.doi.org/10.1063/1.4895903
View Table of Contents: http://scitation.aip.org/content/aip/journal/jcp/141/12?ver=pdfcov
Published by the AIP Publishing

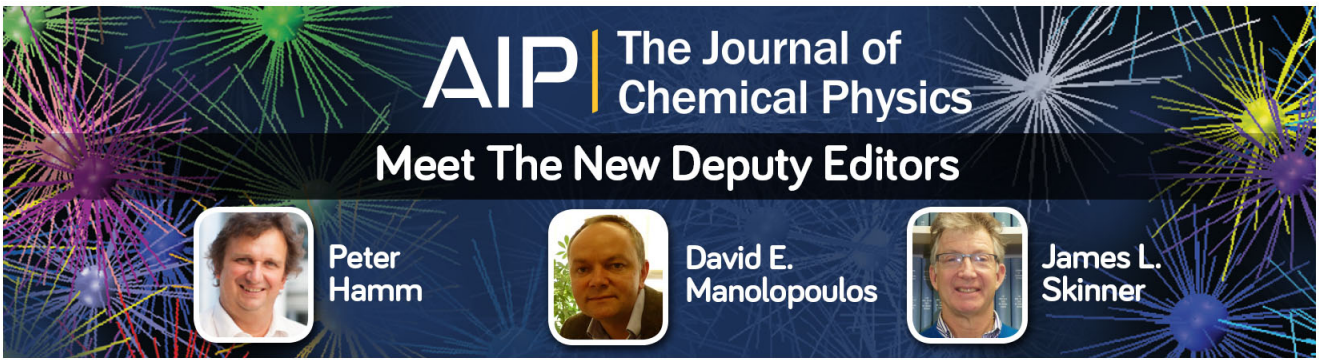

Elastic differential cross sections for C_4F_6 isomers in the 1.5–200 eV energy electron impact: Similarities with six fluorine containing molecules and evidence of F-atom like scattering

M. Hoshino,[1] P. Limão-Vieira,[1,2,a)] K. Anzai,[1] H. Kato,[1] H. Cho,[3] D. Mogi,[4] T. Tanioka,[5] F. Ferreira da Silva,[2] D. Almeida,[2] F. Blanco,[6] G. García,[7] O. Ingólfsson,[8] and H. Tanaka[1]
[1]*Department of Physics, Sophia University, Chiyoda-ku, Tokyo 102-8554, Japan*
[2]*Laboratório de Colisões Atómicas e Moleculares, CEFITEC, Departamento de Física, Faculdade de Ciências e Tecnologia, Universidade Nova de Lisboa, 2829-516 Caparica, Portugal*
[3]*Department of Physics, Chungnam National University, Daejeon 305-764, South Korea*
[4]*Research and Marketing Management Dept., New Products Development Div., Kanto Denka, Kogyo Co., Ltd., Chiyoda-ku, Tokyo 101-0063, Japan*
[5]*Shibukawa Development Research Lab., New Products Development Div., Kanto Denka Kogyo Co., Ltd., Shibukawa City, Gunma 377-8513, Japan*
[6]*Departamento de Física Atómica, Molecular y Nuclear, Universidad Complutense de Madrid, Avenida Complutense, 28040 Madrid, Spain*
[7]*Instituto de Física Fundamental, Consejo Superior de Investigaciones Científicas (CSIC), Serrano 113-bis, 28006 Madrid, Spain*
[8]*Department of Chemistry, Science Institute, University of Iceland, 107 Reykjavik, Iceland*

(Received 2 July 2014; accepted 4 September 2014; published online 22 September 2014)

We report absolute elastic differential cross sections for electron interactions with the C_4F_6 isomers, hexafluoro-1,3-butadiene (1,3-C_4F_6), hexafluoro-2-butyne (2-C_4F_6), and hexafluorocyclobutene (c-C_4F_6). The incident electron energy range is 1.5–200 eV, and the scattered electron angular range for the differential measurements varies from 15° to 150°. In all cases the absolute scale of the differential cross section was set using the relative flow technique, with helium as the reference species. Atomic-like behaviour in these scattering systems is shown here for the first time, and is further investigated by comparing the elastic cross sections for the C_4F_6 isomers with other fluorinated molecules, such as SF_6 and C_nF_6 (n = 2, 3, and 6). We note that for all the six-F containing molecules, the scattering process for electron energies above 30 eV is indistinguishable. Finally, we report results for calculations of elastic differential cross sections for electron scattering from each of these isomers, within an optical potential method and assuming a screened corrected independent atom representation. The level of agreement between these calculations and our measurements is found to be quite remarkable in all cases. © *2014 AIP Publishing LLC*. [http://dx.doi.org/10.1063/1.4895903]

I. INTRODUCTION

In this paper we report absolute elastic differential cross sections (DCSs) for electron interactions with the C_4F_6 isomers, hexafluoro-1,3-butadiene (1,3-C_4F_6), hexafluoro-2-butyne (2-C_4F_6), and hexafluorocyclobutene (c-C_4F_6), and compare these with four other molecules containing six fluorine atoms, i.e., C_6F_6, SF_6, and C_nF_6 (n = 2 and 3). This is the third part of our study into the scattering dynamics in electron collisions with these compounds. Our first contribution[1] dealt with a comprehensive study into electronic excitation to the singlet states of the C_4F_6 isomers by electron energy-loss spectroscopy and *ab initio* calculations, while our second contribution[2] addressed the role of low-lying triplet states in the dissociation mechanism behind the formation of CF_x radicals from these compounds, which is a topic with particular relevance for plasma etching.

In a recent review, Yoon and co-workers[3] presented a collection of elastic differential, integral, and momentum transfer cross sections for electron-polyatomic molecule collisions for 17 molecular species relevant to plasma processing. In this work, also a comprehensive survey of previous experimental and theoretical electron scattering studies for these polyatomic molecules is given. Among the molecules reported by Yoon and co-workers[3] are C_6F_6, SF_6, and C_nF_6 (n = 2 and 3). These all exhibit very different molecular properties but at the same time they all have in common that they contain six fluorine atoms. A comparison of the DCSs reported for these molecules with the DCSs measured here for the C_4F_6 isomers is thus well suited as a measure for the validity range of the IAM (Independent Atom Model) approximation.

To our knowledge, the only previous experimental work on electron scattering from 1,3-C_4F_6 and 2-C_4F_6 is grand total cross section (TCS) measurements by Szmytkowski and Kwitnewski[4,5] covering the energy range from 0.5 to 370 eV. In Table I we summarize the dipole moment and polarizability for C_4F_6 isomers together with these for SF_6, C_6F_6, and C_nF_6 (n = 2 and 3). While 1,3-C_4F_6 and 2-C_4F_6

a)Author to whom correspondence should be addressed. Electronic mail: plimaovieira@fct.unl.pt. Tel.: (+351) 21 294 78 59. Fax: (+351) 21 294 85 49.

TABLE I. A summary of some of the important physicochemical properties of the C_4F_6 isomers, 1,3-C_4F_6, 2-C_4F_6, and c-C_4F_6. Also included are the dipole polarizabilities of F, SF_6, C_2F_6, C_3F_6, and C_6F_6.

	Property			Property	
Species	Dipole moment (D)	Dipole polarizability (10^{-24} cm^3)	Species	Dipole moment (D)	Dipole polarizability (10^{-24} cm^3)
1,3-C_4F_6	0	8.345[a]	F	...	0.557[b]
2-C_4F_6	0	7.73[a]	SF_6	0	6.54[b]
c-C_4F_6	1.345[c]	7.414[a]	C_2F_6	0	4.848[a], 6.82[b]
			C_3F_6	0.4[d]	6.596[b]
			C_6F_6	0	9.58[a], 10.393[b]

[a]www.chemspider.com.
[b]CRC Handbook of Chemistry and Physics, edited by W. M. Haynes, 92nd ed. (CRC, New York, 2011–2012).
[c]L.-W. Xu, M. E. Klausner, A. M. Andrews, and R. L. Kuczkowski, J. Phys. Chem. A **97**, 10346 (1993).
[d]C. A. Mertdogan, T. P. DiNoia, and M. A. McHugh, Macromolecules **30**, 7511 (1997).

have no dipole moments and c-C_4F_6 shows a rather modest value (Table I), all these compounds have dipole polarizabilities of considerable magnitude. Thus, we may anticipate that the main factor determining the angular and energy dependent behaviour of the intermediate-energy electron-scattering cross sections for these compounds is the polarization effect.

In a recent work on elastic electron scattering from the halomethane molecules CH_3X (X = F, Cl, Br, and I),[6] atomic-like behaviour of these scattering systems was clearly demonstrated for the first time by comparing the elastic cross sections of such molecules with those reported for the corresponding noble gases Ne, Ar, Kr, and Xe, respectively. Moreover, Limão-Vieira *et al.*[7] have, soon after, demonstrated atomic-like behaviour of the CCl_4 scattering system by comparison of the elastic cross sections at intermediate impact energies with these for chloromethane (CH_3Cl) and atomic chlorine.[6] Nevertheless, it has been suggested that the charge distribution of the electrons in the target molecule plays an important role in the energy range that was considered, i.e., 50–200 eV. In both studies,[6,7] optical potential calculations, assuming an independent atom configuration including screening corrections for larger molecules (IAM-SCAR),[8,9] have been employed. We note that this represented the first such theoretical data to become available in the literature for those scattering systems.

The present study represents a new and original experimental contribution for the measurement of elastic differential cross section data for C_4F_6 isomers and their comparison with other six-F containing molecules. Here, we are aiming to show that the scattering process, generally speaking above 30 eV, is not sensitive to the nature of the inner atomic constituents but rather to the outer, i.e., in the electron-molecule scattering process, atoms being shielded by outer ones do not contribute to the molecular cross section. In Sec. II we provide details on the experimental apparatus and the measurement techniques that have been used. In Sec. III, we present a brief discussion on the theoretical approach as well on the fitting and integration methods used and in Sec. IV the experimental results are presented together with a discussion and comparison with other results, where that is possible. Finally, some conclusions that can be drawn from this study are given in Sec. V.

II. APPARATUS AND OPERATING PROCEDURES

Two different crossed-beam electron spectrometers were used in the present work. One was used for low-impact energies and high resolution (EELS-1) and the other for energies above 50 eV and low resolution (EELS-2). Both spectrometers have been described in detail before,[6,10] so only a brief description will be given here. A monochromatic electron beam is generated with a hemispherical electron monochromator and crossed at right angles with an effusive molecular beam that enters the interaction region through a 5 mm long capillary with a 0.3 mm inner diameter. After electron interaction with the target gas, the scattered electrons are energy analysed with a hemispherical electron analyser, which can be rotated around the gas jet, and detected with an electron multiplier. Both the electron monochromator and the energy analyser are enclosed in separate, differentially pumped housings. This greatly reduces the effect of background gases and improves the stability of the spectrometer, particularly when reactive gases are being studied. The typical base pressure in the main chamber was 1.0×10^{-5} Pa and, upon gas admission, increased to 1.0×10^{-4} Pa. In order to reduce any possible contamination during measurements, the spectrometer and molecular beam source are heated to a temperature of about 55 °C. The 1,3-C_4F_6 gas sample was supplied from Kanto Denak Kogyo Co., Ltd. and 2-C_4F_6 and c-C_4F_6 were supplied by Hydrus Chemical Inc. The stated purity was 99.9% for 1,3-C_4F_6 and 98% for 2-C_4F_6 and c-C_4F_6, respectively. All substances were used as delivered.

In the current experiments the energy resolution of the incident electron beam was 35-45 meV and 80-100 meV (FWHM), for EELS-1 and EELS-2, respectively. Correspondingly, the electron current of the former was typically few nA and that of the latter, 30-40 nA (depending on the initial electron energy). Due to the finite resolution of these instruments there could, in principle, be contributions to the elastic signal from some of the lower-lying vibrational modes of C_4F_6. In the energy range above 10 eV, however, such vibrational contributions are expected to be very small compared to the elastic intensity, and thus are not expected to make any significant contribution to the measured elastic cross sections. Above 10 eV incident electron energy, we thus do not make any effort to extract these contributions. Below 10 eV, however, the

energy loss spectra have been deconvoluted with Gaussian profiles representing the lower-lying vibrational modes of C_4F_6 to separate these from the elastic DCSs (not shown here). The incident electron energy was calibrated with respect to the 19.365 eV, ^2S resonance in He,[11] and with respect to the $^2\Pi_g$ resonance in N_2 for the vibrational excitations around 2.4 eV.[12] The hemispherical electron analyser is placed on a turntable stage and can be rotated from -10° to $+130^\circ$ for EELS-1 and from -10° to $+150^\circ$ for EELS-2, with respect to the incident electron beam. The angular resolution is about $\pm 1.5^\circ$ in both instruments.

The absolute scale of the present DCSs was set using the relative flow technique,[13] in which the ratio of the elastic scattering intensity for the C_4F_6 molecules to that of helium under the same experimental conditions was determined. Then employing the known helium elastic DCSs, as reported in Boesten and Tanaka,[14] we can derive the respective DCSs. We estimate that the experimental uncertainties on the resulting C_4F_6 DCSs lie in the range of 15%–20%, with the actual value depending on the specific incident electron energy (E_0) and scattered electron angle (θ) under consideration. This overall error is largely comprised of the uncertainty in the reference helium DCSs, and the uncertainty arising from the gas flow conditions for the relative flow technique. To a much lesser extent uncertainty arising from the statistical accuracy of the data and the fluctuation in the current of the incident electron beam is negligible (<1%).

III. THEORETICAL APPROACH (IAM-SCAR), FITTING AND INTEGRATION METHODS

Details of the application of the IAM-SCAR[8,9] method to electron interactions have been provided in a number of previous papers (see, e.g., Refs. 6 and 7). Briefly, each atomic target (C, F) is represented by an interacting complex potential (the so-called optical potential). The real part accounts for the elastic scattering of the incident electrons, and the imaginary part represents the inelastic processes, which are considered as "absorption" from the incident beam. For the elastic part, the potential is represented by the sum of three terms: (a) a static term derived from a Hartree–Fock calculation of the atomic charge density distribution, (b) an exchange term to account for the indistinguishability of the incident and target electrons, and (c) a polarization term for the long-range interactions which depends on the target polarizability α (see Table I). The inelastic scattering, on the other hand, is treated as electron-electron collisions. Further improvements to the original formulation in the description of the electron's indistinguishability and the inclusion of screening effects led to a model which provides a good approximation for electron-atom scattering over a broad energy range. To calculate the cross sections for electron collisions with C_4F_6 isomers, the additivity rule (AR) is then applied to the optical model results for each constituent atom. In this approach, the molecular scattering amplitude stems from the sum of all the relevant atomic amplitudes, including the phase coefficients, which gives the DCSs for the molecule of interest. Integral cross sections (ICSs) can then be determined by integrating those DCSs. The geometry of the molecule (atomic positions and bond lengths) is taken into account by using some screening coefficients and this enables the range of validity of the technique to be extended down to impact energies of ~30 eV (or lower) for electron scattering.

The measured elastic DCS were extrapolated ($\theta < 15^\circ$ and $\theta > 130^\circ$) with the help of a fitting method and then integrated numerically. Briefly, we have made use of a modified phase shift analysis (PSA) (see Eqs. (1)–(3)), including polarization and the Born approximation for the higher phase shifts (Eq. (3)), or the corresponding shapes of our IAM-SCAR calculation as a guide (see, e.g., Refs. 6–9 and references therein for details on the calculation procedure). As far as the modified PSA is concerned, briefly, the fitting formulas were used by a single expression as

$$d\sigma(\theta)/d\Omega = |f(\theta)|^2 \tag{1}$$

and

$$2ikf(\theta) = N(k)\left\{\sum_{\ell=0}^{L}[S_\ell(k)-1](2\ell+1)P_\ell(\cos\theta)+C_L(\theta)\right\} \tag{2}$$

with

$$C_L(\theta) = 2i\pi\alpha k^2\left\{\frac{1}{3} - \frac{1}{2}\sin(\theta/2) - \sum_{\ell=1}^{L} P_\ell(\cos\theta)/(2\ell+3)(2\ell-1)\right\}, \tag{3}$$

where C_L is the Born approximation for the higher phases in the Thompson form,[15] k is the wave number of the free electron, α is the atomic/molecular polarizability, P_ℓ is the Legendre polynomials, and $f(\theta)$ is the scattering amplitude. Values of α relevant to this study can be found in Table I. In simple PSA fitting,[16] $N(k) = 1$, and the scattering function becomes $S_\ell(k) = \exp(2i\delta_\ell)$, where δ_ℓ are the phase shifts. As shown in Figs. 1(a)–1(c), the present PSA fitting results typically follow theory in the unaccessed DCS angular regions up to an impact energy of 10 eV. The parameter L is set to be as small as possible (generally less than 5) being limited by the number of experimental points and the degree of smoothing. At low energies k^2 makes the fit nearly independent of α. Therefore, above 10 eV, the shape of the IAM-SCAR theory is more reliable to help obtaining the integral cross section. This is reasonable as the calculation is in good agreement with the experiment over the range of angles measured for the DCS at these energies, as discussed in more detail in Sec. IV. Due to the uncertainty involved in the extrapolation process, we estimate an error of ~30% of the present elastic ICSs and momentum transfer cross sections (MTCSs).

IV. RESULTS AND DISCUSSION

Table I summarizes the dipole moments and dipole polarizability of the C_4F_6 isomers, 1,3-C_4F_6, 2-C_4F_6, and c-C_4F_6, together with F, SF_6, C_2F_6, C_3F_6, and C_6F_6. Though the present C_4F_6 isomers are six-fluorine containing molecules where the constituent carbons are composed with mutually different configurations, i.e., cis-, linear-, and cyclic-structures. Tables II–IV list the measured DCS for electron

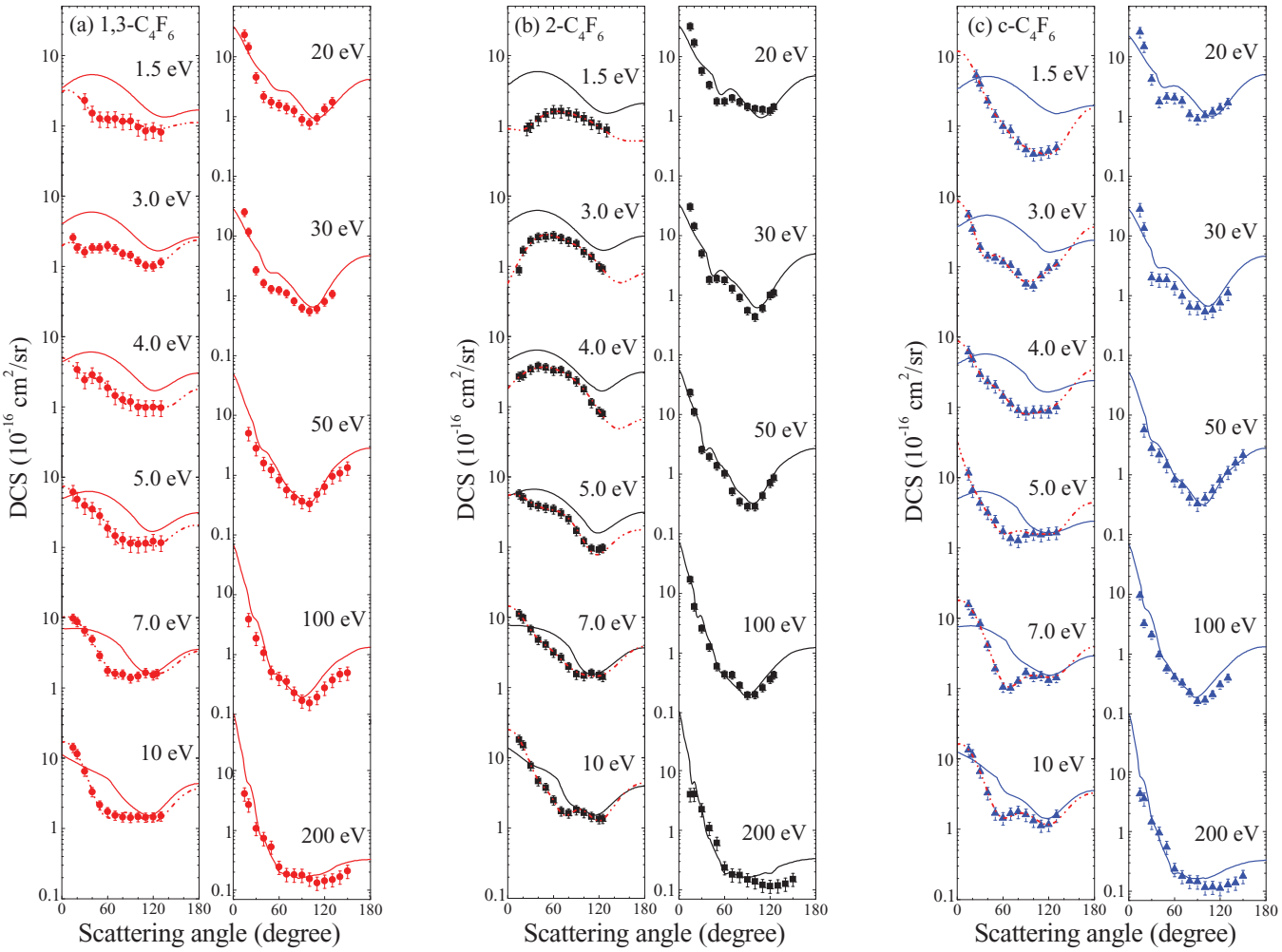

FIG. 1. The elastic DCSs (10^{-16} cm^2/sr) for electron scattering from (a) 1,3-C_4F_6, (b) 2-C_4F_6, and (c) c-C_4F_6 in the energy range of 1.5–200 eV. Solid curves: the present IAM-SCAR calculations. Dotted-dashed curves: the results from our modified PSA fitting.

TABLE II. Present elastic DCSs (10^{-16} cm^2/sr) for electron scattering from 1,3-C_4F_6. The current ICSs and MTCSs (both in units of 10^{-16} cm^2), derived from present DCSs, are given at the foot of the table.

	Impact energy (eV)										
Angle (deg)	1.5	3.0	4.0	5.0	7.0	10	20	30	50	100	200
15	…	2.545	…	6.097	9.707	14.09	23.26	25.00	…	…	4.103
20	…	1.833	3.392	4.815	8.659	11.39	14.28	11.79	5.021	3.870	2.690
30	2.292	1.587	2.412	3.931	6.457	6.447	4.541	2.662	2.801	1.868	1.081
40	1.522	1.832	2.872	3.476	4.844	3.301	2.160	1.628	1.595	1.066	0.737
50	1.265	1.834	2.431	2.808	2.857	2.145	1.743	1.297	1.221	0.513	0.530
60	1.259	1.959	1.865	1.870	1.747	1.726	1.563	1.245	0.825	0.404	0.243
70	1.269	1.772	1.439	1.461	1.589	1.537	1.394	1.100	0.563	0.352	0.185
80	1.168	1.498	1.269	1.292	1.564	1.447	1.244	0.813	0.429	0.229	0.181
90	1.174	1.428	1.183	1.137	1.375	1.424	0.896	0.625	0.635	0.168	0.178
100	0.959	1.177	1.003	1.112	1.461	1.463	0.769	0.551	0.330	0.154	0.155
110	0.844	1.024	0.977	1.140	1.633	1.439	0.929	0.601	0.478	0.193	0.132
120	0.890	1.007	0.989	1.224	1.523	1.444	1.339	0.796	0.640	0.276	0.143
125	…	…	…	…	1.589	…	…	…	…	…	…
130	0.814	1.136	0.972	1.164	…	1.495	1.737	1.069	0.955	0.372	0.150
140	…	…	…	…	…	…	…	…	1.080	0.469	0.167
150	…	…	…	…	…	…	…	…	1.329	0.491	0.209
ICS	15.218	19.048	19.610	23.369	31.413	31.417	34.063	28.850	18.170	9.681	7.269
MTCS	13.072	17.570	15.381	17.680	23.403	22.554	23.319	15.763	13.891	4.598	2.306

TABLE III. Present elastic DCSs (10^{-16} cm^2/sr) for electron scattering from 2-C_4F_6. The current ICSs and MTCSs (both in units of 10^{-16} cm^2), derived from present DCSs, are given at the foot of the table.

	Impact energy (eV)										
Angle (deg)	1.5	3.0	4.0	5.0	7.0	10	20	30	50	100	200
15	...	0.874	2.672	5.649	11.11	18.04	32.15	30.42	23.33	17.10	4.009
20	...	1.666	2.812	5.009	9.667	15.02	17.17	14.39	11.11	5.975	4.034
25	0.906	...	...	...	...	...	...	...	...	...	...
30	1.004	2.310	3.390	4.074	6.688	7.677	5.772	5.030	2.572	2.581	2.244
40	1.252	2.585	3.750	3.850	4.768	4.655	3.358	1.811	1.970	1.263	1.085
50	1.446	2.635	3.580	3.632	4.056	3.746	1.779	1.900	1.380	0.597	0.613
60	1.610	2.700	3.278	3.471	3.144	2.480	1.772	1.783	1.022	0.439	0.238
70	1.619	2.500	3.285	3.034	2.653	1.735	2.019	1.287	0.516	0.429	0.181
80	1.503	2.271	2.809	2.517	1.970	1.623	1.733	0.917	0.347	0.286	0.176
90	1.433	2.075	2.300	1.700	1.540	1.805	1.453	0.551	0.286	0.198	0.15
100	1.281	1.590	1.761	1.206	1.467	1.637	1.338	0.432	0.286	0.201	0.138
110	1.109	1.350	1.136	0.950	1.600	1.445	1.290	0.607	0.435	0.263	0.12
120	0.981	0.994	0.853	0.916	1.509	1.342	1.236	1.000	0.708	0.363	0.116
125	...	0.915	0.788	0.970	1.417	1.358	1.431	1.099	0.870	0.429	...
130	0.875	...	...	...	...	...	...	...	...	...	0.118
140	...	...	...	...	...	...	...	...	...	...	...0.126
150	...	...	...	...	...	...	...	...	...	...	0.152
ICS	14.878	21.817	26.559	28.544	36.824	39.462	42.906	29.578	24.981	16.413	7.514
MTCS	13.392	17.326	18.637	20.090	26.531	26.361	26.606	16.498	12.318	6.280	2.310

scattering from the C_4F_6 isomers. At the bottom of Tables II–IV the elastic ICSs and MTCSs are also given.

Figures 1(a)–1(c) illustrate the angular distributions of the current DCSs for 1,3-C_4F_6, 2-C_4F_6, and c-C_4F_6, respectively, together with the corresponding results from the IAM-SCAR computations and the results from the modified PSA fitting. Figure 2 compares the experimental elastic DCS of these C_4F_6 isomers at 3, 7, and 10 eV incident electron energies and also shows the IAM-SCAR calculations. In Figure 3 the measured DCS for C_4F_6 isomers, C_nF_6 (n = 2, 3, and 6) and SF_6 are compared at 50 and 100 eV, respectively, along with the corresponding theoretical results from the IAM-SCAR model for the F and C atoms. Finally, the experimental and theoretical elastic ICSs for 1,3-C_4F_6, 2-C_4F_6, and c-C_4F_6, are plotted in Fig. 4, respectively, along with available experimental and theoretical literature data on the total cross sections,[5] and experimental data on the ionization[17] and attachment cross sections.[18] Note, as mentioned above, that

TABLE IV. Present elastic DCSs (10^{-16} cm^2/sr) for electron scattering from c-C_4F_6. The current ICSs and MTCSs (both in units of 10^{-16} cm^2), derived from present DCSs, are given at the foot of the table.

	Impact energy (eV)										
Angle (deg)	1.5	3.0	4.0	5.0	7.0	10	20	30	50	100	200
15	...	5.451	6.129	11.516	15.470	13.311	25.748	46.74	...	9.560	4.304
20	...	3.408	4.727	6.508	11.740	11.154	14.725	22.29	5.691	3.245	3.536
25	5.208	...	...	...	...	...	...	...	...	...	...
30	3.920	1.881	2.920	4.284	8.300	6.614	4.185	3.291	2.777	2.089	1.450
40	2.251	1.401	2.295	3.155	4.084	3.251	1.756	3.092	2.155	0.972	0.943
50	1.418	1.316	1.991	2.415	1.904	1.682	2.090	3.099	1.439	0.565	0.550
60	0.986	1.164	1.435	1.691	1.042	1.430	2.046	2.285	0.832	0.410	0.234
70	0.859	1.039	1.122	1.356	1.013	1.671	1.783	1.629	0.660	0.328	0.178
80	0.588	0.812	0.899	1.265	1.268	1.763	1.070	1.076	0.411	0.227	0.147
90	0.461	0.566	0.826	1.513	1.688	1.600	0.900	1.051	0.328	0.162	0.144
100	0.397	0.529	0.877	1.593	1.470	1.320	1.033	0.893	0.405	0.170	0.116
110	0.408	0.740	0.881	1.525	1.519	1.122	1.186	0.952	0.542	0.210	0.118
120	0.437	0.943	0.876	1.607	1.305	1.162	1.384	1.266	0.805	0.305	0.112
130	0.492	1.089	1.011	1.640	1.415	1.556	1.693	1.836	1.110	0.396	0.129
140	...	...	...	...	...	...	...	...	1.587	...	0.139
150	...	...	...	...	...	...	...	...	2.118	...	0.179
ICS	15.979	16.469	19.851	30.985	32.459	30.414	35.981	28.842	18.597	11.221	7.729
MTCS	9.040	15.025	16.423	25.421	22.610	21.505	24.847	15.723	14.073	5.137	2.307

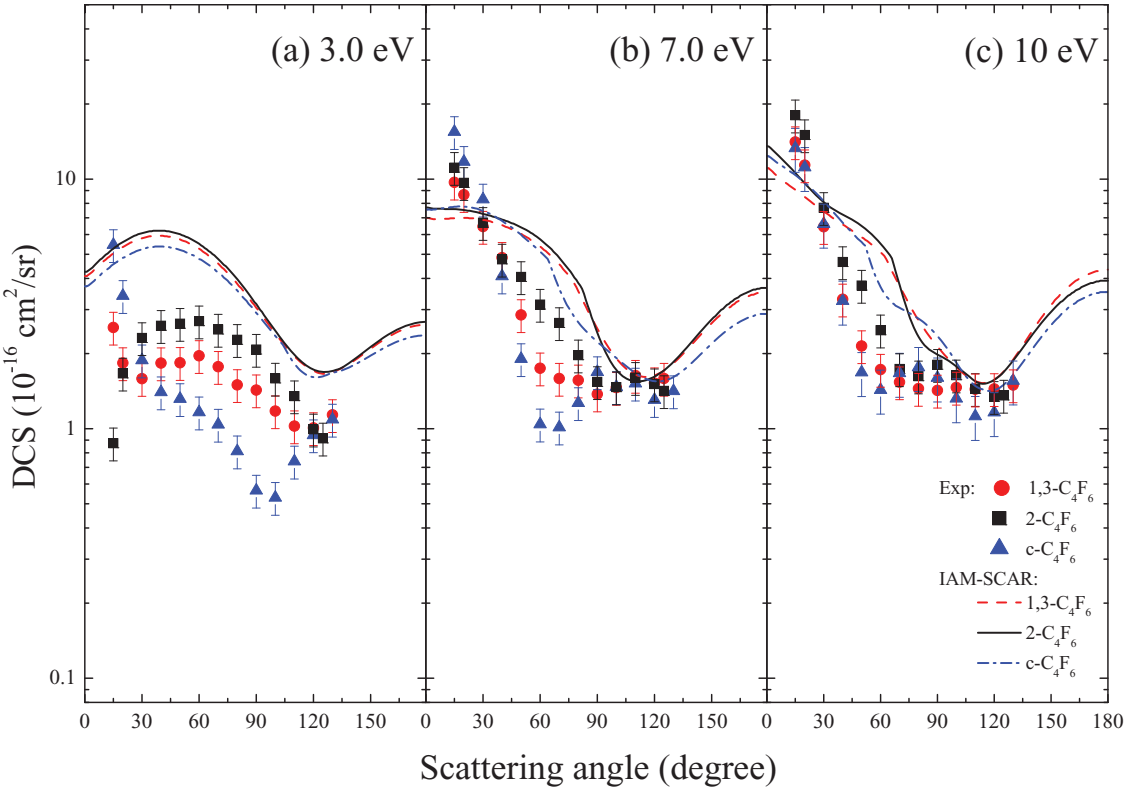

FIG. 2. A comprehensive comparison between the experimental elastic DCSs for the C_4F_6 isomers together with the IAM-SCAR calculations. Data at representative incident energies are shown for (a) 3.0 eV, (b) 7.0 eV, and (c) 10 eV.

there is no previous theoretical data on the C_4F_6 isomers available for comparison except from the present calculation. We will now discuss the main relevant features from the analysis of each figure.

A. Elastic DCS overview

The first systematic and concise set of data for electron scattering from 1,3-C_4F_6, 2-C_4F_6, and c-C_4F_6 are presented

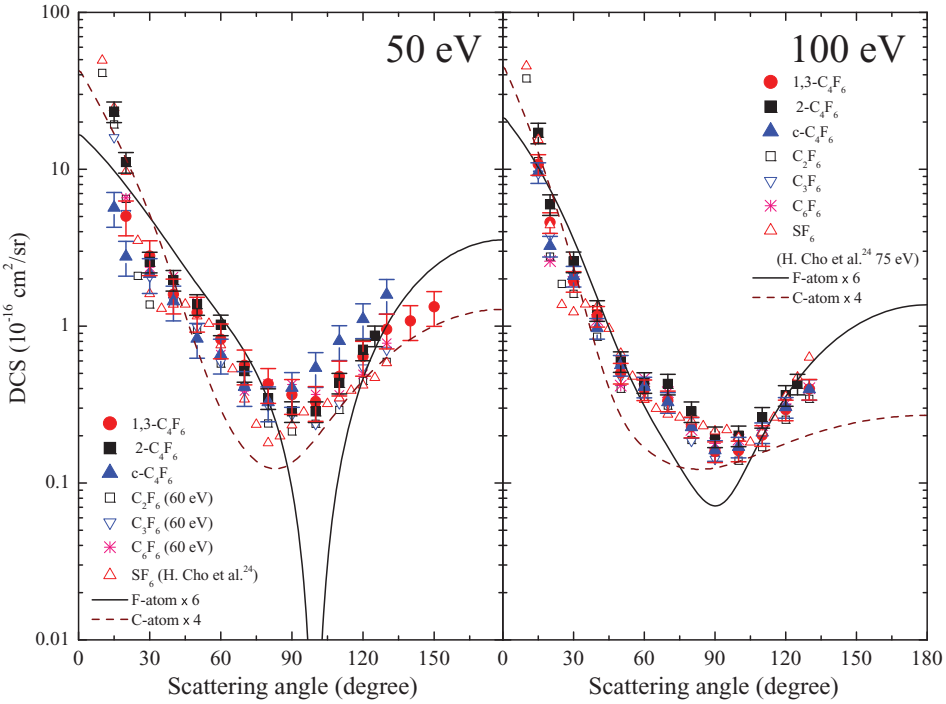

FIG. 3. A comparison between the elastic DCSs of C_4F_6 isomers, at 50 and 100 eV, C_nF_6 (n = 2, 3, and 6) at 60 and 100 eV and SF_6 at 50 and 75 eV, respectively. Also included are theoretical results from our IAM-SCAR calculations for 6 atomic fluorines (DCS of a fluorine atom multiplied by 6) and 4 atomic carbons (DCS of a carbon atom multiplied by 4).

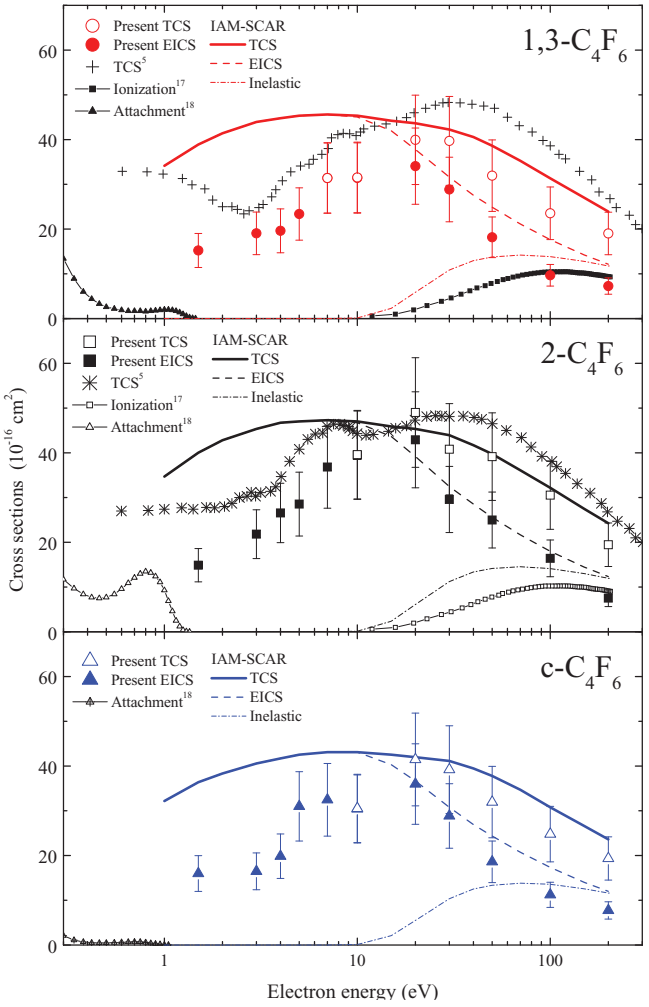

FIG. 4. Elastic ICS for 1,3-C_4F_6 (●) and ICS plus inelastic cross sections (○), for 2-C_4F_6 (■) and (□), for c-C_4F_6 (▲) and (△), compared against our elastic IAM-SCAR ICS (dashed line), our total IAM-SCAR cross sections (solid line), and our IAM-SCAR ICS for total inelastic processes (dashed-dotted line). Also shown other total cross sections,[5] ionization,[17] and attachment cross sections.[18] See text for details.

in the energy range from 1.5 to 200 eV, and over the scattering angle range between 15° and 150°. It is clear from Figs. 1(a)–1(c) that the measured DCSs are generally strongly peaked in magnitude towards forward scattering angles. This effect is, however, less pronounced for 1,3-C_4F_6 below 5 eV and for 2-C_4F_6 at electron energies below 5 eV. This result is consistent with the long-range interactions and it is worth noting that 1,3-C_4F_6 and 2-C_4F_6 have no permanent dipole moments and that of c-C_4F_6 is relatively small, while all three are more susceptible to the dipole polarizability at lower impact energies (Table I). The DCSs measured at 100–200 eV show the strongest enhancement, which is reminiscent of direct scattering from the long-range polarization potential being the most dominant interaction mechanism at higher impact energies. Another interesting characteristic is the absence of any observable effect from the different molecular compositions of these compounds on the measured DCSs at higher energies, i.e., DCSs show remarkable similarities with six fluorine containing molecules above about 20 eV. At 100 and 200 eV, DCSs are undulated moderately for the forward scattering direction due to the interference of the scattering waves from the composite atoms. Those features are clearly reflected in the IAM-SCAR calculations which agree particularly well with the measured DCSs, at higher impact energies.

Within the IAM-SCAR framework described above, the electron-molecule interaction potential is basically assumed to be a coherent sum of spherical atomic potentials, so the angular distribution of the elastic scattering (DCS) depends on the chemical binding, i.e., cis-, linear-, and cyclic-molecular structures, resulting in a considerable anisotropic charge distribution of the valence electrons for the C_4F_6 isomers. However, we calculated the cross sections by assuming random orientations because this is the normal situation of the experiments in the gas phase. Furthermore, due to the optical theorem, the ICSs are always the sum of the atomic ones. The effect of the SCAR corrections is to reduce the contribution of the atomic cross sections when they overlap (i.e., at the lower energies). This approximation has been, however, applied successfully: (1) if the constituent atoms in the target are heavy atoms[23] and (2) if the interaction region is the inner part of each atom for fast electrons large-angle scattering,[7] where the potential field is more or less spherical. Even so, at 200 eV for C_4F_6 isomers, some deviations are emerging commonly for backward scattering above 90°, which may be due to the multiple scattering processes in a molecule. However, the present computation describes reasonably well, both qualitative and quantitatively speaking, the cross sectional behaviour above 20 eV.

Hence, below 20 eV, electron interactions may be more dominated by the chemical-binding molecular nature. As discussed below, DCSs reveal more complicated but systematic trend both in the angular distributions and in the magnitudes, which cannot be reproduced with the present IAM-SCAR calculations. Its limit of application will motivate more sophisticated approaches, like R-matrix, the Schwinger Multichannel methods to try to describe those features. Typically below 20 eV, electron interactions may be resonant in character, leading to the formation of transient negative ions (TNIs) through electron attachment, i.e., shape resonance. Such TNIs may decay in the elastic or inelastic channel but may also lead to a metastable anion or to dissociation of the molecule (dissociative electron attachment) producing neutral products and fragment anions.[19–21] At low electron impact energies, C_4F_6 isomers exhibit resonance features in the TCSs between 1 and 15 eV, as most noticeable in Fig. 4 for 1,3-C_4F_6 and 2-C_4F_6 in the incident energy range between 2 and 10 eV. Such characteristics are, in general, expected to be predominantly both in the elastic scattering and, notably, in the vibrational inelastic channels, but dissociative electron attachment may also contribute.

Furthermore, below 20 eV in Fig. 1, DCSs are extrapolated in the forward and backward directions with the help of a modified PSA fitting just as a guide because of no theoretical calculations available in the literature. Note, in practice, this fitting is used for smoothing (e.g., interpolating) the DCS measured, while the contribution from the extrapolated DCSs is within less than 10% over all scattering angles (in the integration due to the weighting factor $\sin\theta$).

1. Elastic DCS of 1,3-C_4F_6

At low impact energies, i.e., in the range from 1.5 to about 5 eV a weak minimum that shifts towards smaller angles with increasing energy is observed in the elastic DCSs of 1,3-C_4F_6 at fairly small scattering angle. Further, a weak maximum at ∼40° becomes noticeable at 4 eV and vanishes at higher energies (already at 7 eV). Such undulation in the angular behaviour results from the scattering attributed to the chemical-binding molecular nature with weak resonant features. It is also worth commenting that at electron impact energies from 5 to 10 eV, above 70°, the measured DCS is fairly isotropic. This may be related to several weak resonant channels opening in this energy range as can be seen on the rising slope of the broad feature at about 5 and 8 eV in the TCS.[4,5] From these, the former may be related to the formation of TNIs, i.e., the temporary trapping of the incident electron in a π_a (20a) → $\pi_b{}^*$ (20b) antibonding molecular orbital, observed in the electron spectra,[1,22] and the latter with higher lying resonances from dissociative electron attachment experiments.[20,21]

At higher energies, the experimental data agrees well with the IAM-SCAR calculation which is reminiscent of the dominant direct scattering in this energy range. Here, the DCSs show a clear minimum at ∼100° at 20, 30, 50, and 100 eV, which slightly shifts to larger angles and becomes shallower at 200 eV. A less pronounced minimum is also apparent at about 40°–50° in the range from 20 to 200 eV and is progressively shifted to larger angle above 30 eV.

2. Elastic DCS of 2-C_4F_6

In contrast to 1,3-C_4F_6, Szmytkowski and Kwitnewski[4,5] noticed that the TCS of 2-C_4F_6 does not show a maximum at very low energies but only one very broad enhancement with two maxima peaking at ∼8 and 30 eV. The latter was reported in other perfluorinated hydrocarbons and attributed to a behaviour in common with perfluorinated compounds.[4,5] This is particularly relevant for discussion in Sec. IV C. The previous electron scattering data,[4,5] reported a shoulder in the TCS between 2.5 and 4.0 eV and peaking somehow at 2.8–3.0 eV, which may also partly be attributed to a resonant electron capture.[20] Around 8 eV, the TCS is characterised by a pronounced maximum[4,5] and we notice in a recent study on the electronic state spectroscopy of the C_4F_6 isomers[1] that hexafluoro-2-butyne shows an intense oscillator strength (at 9.94 eV) assigned to the A_{2u} component of the π ($6e_u$) → π^* ($6e_g$) transition.

The most noticeable feature in the experimental DCSs of 2-C_4F_6 is the strong forward scattering at higher energies and how this gives way to a relatively isotropic DCS at 7 and 10 eV. Below 4 eV the cross section decreases as the angle becomes smaller. This is evocative of the behaviour noted previously[6] in a number of molecules at energies near or above the position of low energy shape resonances (in the vicinity of 2 eV in electron attachment to 2-C_4F_6). Also, at about 3 eV a maximum at ∼30° becomes noticeable but vanishes as the impact energy increases (already at 5 eV).

Above 10 eV the experimental DCSs for 2-C_4F_6 agree well with the IAM-SCAR calculations and besides the strong forward scattering component the main features are two minima, one close to 45° at 20 eV that is progressively shifted to shorter angles with increasing energy, and a second at ∼100° at 30, 50, and 100 eV that is shifted to larger angles at 200 eV.

3. Elastic DCS of c-C_4F_6

The general shapes of the DCSs of hexafluorocyclobutene may be divided into the low energy regime where resonant processes can contribute significantly and the higher energy regime where direct scattering dominates. In particular, the DCSs show a clear minimum at 3 eV (∼40° scattering angle) that shifts towards larger scattering angles at 4 eV and vanishes at about 5 eV. A new minimum starts to evolve at 5 eV and becomes more pronounced at 7 eV, and is shifted towards smaller angles, at 7 and 10 eV. Also, it is noticeable that at 4, 5, and 7 eV incident electron energy the measured DCS is fairly isotropic above 80° scattering angle. In a recent electron energy loss spectroscopy study,[1] an intense feature which has been assigned to the π ($7b_1$) → $\pi^*{}_{C=C}$ ($1a_2$) transition was observed in this energy region. This contribution was found to peak at 8.02 eV and might, thus, be partly responsible for the isotropy observed in this energy range.

Above 10 eV, the general behaviour of the elastic DCS of c-C_4F_6 is very similar to that of the other C_4F_6 isomers. The agreement with the IAM-SCAR calculations is again good in this energy range and two minima are observed; one at scattering angles at about 30° and the second close to 100°. Similar to the other compounds, the latter minimum is observed close to 100° at 30, 50, and 100 eV impact energies, and gets shallower and is shifted to larger angle at 200 eV.

4. Comparison of C_4F_6 isomers DCS at low and intermediate energies

In Figure 2 we show for comparison the experimental DCS for electron scattering from 1,3-C_4F_6, 2-C_4F_6, and c-C_4F_6 at low and intermediate impact energies, respectively. From Fig. 2, we see clear differences in the DCS behaviour for the C_4F_6 isomers, especially with respect to c-C_4F_6 compared to 1,3- and 2-C_4F_6 at impact energy of 3 eV. At the most forward scattering, only the c-C_4F_6 DCS shows a considerable enhancement, which is almost an order of magnitude larger than in the case of 2-C_4F_6. From Table I we note that, although there is no particular difference between the dipole polarizabilities of the C_4F_6 isomers, the modest dipole moment of c-C_4F_6 may be responsible for the differences in shape and magnitude of the DCS. Regarding Fig. 2 and electron impact energy of 7 eV, with the exception for 60° scattering angle, the general behaviour on the DCSs is identical, and so the clear minimum for c-C_4F_6 can be due to molecular structural differences, i.e., its cyclic form. Of relevance is the fact that from Fig. 1(c) it is clear that for 10 eV (also visible at 7 eV), the c-C_4F_6 isomer shows a considerable undulation enhancement in the DCS which may reflect the cyclic molecular structure contributing to such angular behaviour. Regarding the IAM-SCAR calculation in Fig. 1(b), at energies

below 30 eV, the method often provides a reasonable shape description for the elastic DCS but overestimates the magnitude.

We now turn to Fig. 3 where a close inspection of the experimental DCSs for the C_4F_6 isomers at impact energies of 50 and 100 eV reveals an independent atomic structure effect for the molecules, i.e., the electron scattering process is only sensitive to the presence of the fluorine atoms that actually dictate the nature of the DCSs. Worth mentioning is that Szmytkowski and Kwitnewski[4,5] noticed that the TCS for 1,3-C_4F_6 and 2-C_4F_6 overlapped nearly above 30 eV. They have suggested that an independent atom approximation, at higher energies, can reasonably reproduce the scattering process. This is shown here for the first time that such assumption is correct and we will discuss that in Sec. IV B.

B. Comparison with the atomic F-DCS

In Fig. 3 we compare in detail the present experimental DCSs for each of the C_4F_6 isomer together with SF_6[24] and C_nF_6 (n = 2, 3, and 6) at 50 eV and 100 eV. From a qualitative perspective, there is excellent agreement in all cases of six-fluorine containing molecules DCSs. In many of the plots in Figs. 1(a)–1(c) we also find very good agreement in terms of the magnitudes of the cross sections between our measured and calculated data. Given that our IAM-SCAR theoretical approach is explicitly built upon scattering from atomic centres, the level of agreement observed in Fig. 3 is a strong evidence in support of the assertion that atomic-like effects remain prevalent in what are fundamentally molecular systems. Moreover, as depicted in Fig. 3, we also compare the experimental DCSs with theoretical elastic scattering DCSs from 6 atomic fluorines (DCS of a fluorine atom multiplied by 6) and 4 atomic carbons (DCS of a carbon atom multiplied by 4) at incident electron energies of 50 and 100 eV, respectively. Again, the angular behaviour in the calculated DCSs is reminiscent of those observed in the six-fluorine containing molecules DCSs. We believe this constitutes further convincing evidence for atomic-like behaviour in the scattering dynamics. Nevertheless there are differences, in particular, in regard to the magnitude of the depths of the critical minima (which is more clear for 50 eV), which suggests to us that 4 carbon atoms and the chemical-binding molecular nature effects are still playing a role here.

In a recent publication,[7] we have compared in detail the experimental data on CCl_4 with the previous experimental DCSs for CH_3Cl and theoretical ones (IAM-SCAR) for the Cl atom at 50 eV and 100 eV. From a qualitative point of view, we observed a good agreement in both cases (but particularly at 50 eV) between measurements and calculations. This has allowed us to suggest strong evidence in support of the assertion that atomic-like effects may remain prevalent in what are fundamentally molecular systems. Moreover, Hoshino *et al.*[23] as a result of progressively substituting a Cl-atom in going from CF_4 to CF_3Cl to CF_2Cl_2 to $CFCl_3$, and to CCl_4, the undulations in the angular distributions have been found to vary in a largely systematic manner, concluding therefore that the elastic scattering process is dominated by the atomic-Cl atoms of the molecules.

Kato *et al.*[6] have concluded that in many cases the structure observed in the CH_3X halomethanes (X = F, Cl, Br, and I) was also partly found in the corresponding noble gas species, suggesting therefore that a bonded halogen atom, F, Cl, Br, and I, behaves somewhat like a Ne, Ar, Kr, and Xe atom, respectively. The bonded halogens are acting like their corresponding noble gas counterparts, because the atomic-like behaviour due to heavy atoms (F, Cl, Br, and I) manifests itself in the measured cross sections.

This constitutes further evidence for atomic-like behaviour in the scattering dynamics in addition to the electron scattering collisional data on C_4F_6 molecules. We also note that in Fig. 2 as we go to lower energies, at least until 7 eV, the data suggests that molecular-like behaviour becomes increasingly important.

C. Comparison of integral and total cross sections

In Fig. 4 we show our elastic integral cross sections for 1,3-C_4F_6, 2-C_4F_6, and c-C_4F_6, respectively, as obtained from our measured DCSs as presented in Sec. III. These are compared with the available total cross sections in the literature. In addition, the results from the present IAM-SCAR calculations for the elastic ICS, total cross sections, and sum over all inelastic ICSs (except vibrational excitations) are also plotted. Note that independent ionisation cross sections[17] are also shown for each species, where available, to illustrate the efficacy of the BEB model approach.

In Fig. 4 we compare the present elastic ICS to corresponding results from Refs. 5, 17, and 18. The present "experimental" TCS are, to within our stated uncertainties, generally found to be in reasonable agreement with our calculated IAM-SCAR TCS for each target. This important self-consistency test at the total cross section level gives us some confidence in the validity of our DCS measurements and the elastic ICS we have derived from them. Note that given the rather coarse energy grid of our measurements, we typically do not reproduce the rich resonance structure observed by Szmytkowski and Kwitnewski.[4,5]

V. CONCLUSIONS

We report experimental elastic differential, integral, and momentum transfer cross sections for electron scattering from C_4F_6 molecules. Corresponding comparison with other six-fluorine containing molecules and recent theoretical differential cross sections from the IAM-SCAR model for F atom have also been discussed. Agreement between these sets of data is generally very good at incident electron energies, in terms of the shapes and angular distributions of the cross sections. The level of agreement reported here suggests that atomic-like behaviour in the scattering process may be of considerable relevance, at least in the energy range above 50 eV. Integral elastic cross sections were also determined and found to be in reasonable good agreement with the results from our IAM-SCAR computations. These elastic ICSs were also found to be nicely consistent with the previous results from TCS measurements of Szmytkowski and Kwitnewski[4,5] as well as our own IAM-SCAR results.

ACKNOWLEDGMENTS

This work was conducted under the support of the Japanese Ministry of Education, Sport, Culture, and Technology. F.F.S. and D.A. acknowledge the Portuguese Foundation for Science and Technology (FCT-MEC) for post-doctoral SFRH/BPD/68979/2010 and SFRH/BPD/99261/2013 grants, respectively, and together with P.L.-V. the PEst-OE/FIS/UI0068/2014 and PTDC/FIS-ATO/1832/2012 grants through FCT-MEC grants. P.L.-V. also acknowledges his Visiting Professor position at Sophia University, Tokyo, Japan. F.B. and G.G. acknowledge the partial financial support from the Spanish Ministerio de Economia y Competitividad (Project No. FIS 2012-31230). This work forms part of the EU/ESF COST Action CM0805 programme "The Chemical Cosmos".

[1]P. Limão-Vieira, K. Anzai, H. Kato, M. Hoshino, F. Ferreira da Silva, D. Duflot, D. Mogi, T. Tanioka, and H. Tanaka, J. Phys. Chem. A **116**, 10529 (2012).
[2]P. Limão-Vieira, D. Duflot, K. Anzai, H. Kato, M. Hoshino, F. Ferreira da Silva, D. Mogi, T. Tanioka, and H. Tanaka, Chem. Phys. Lett. **574**, 32 (2013).
[3]J.-S. Yoon, M.-Y. Song, H. Kato, M. Hoshino, H. Tanaka, M. J. Brunger, S. J. Buckman, and H. Cho, J. Phys. Chem. Ref. Data **39**, 033106 (2010), and references therein.
[4]C. Szmytkowski and S. Kwitnewski, J. Phys. B **36**, 2129 (2003).
[5]C. Szmytkowski and S. Kwitnewski, J. Phys. B **36**, 4865 (2003).
[6]H. Kato, T. Asahina, H. Masui, M. Hoshino, H. Tanaka, H. Cho, O. Ingólfsson, F. Blanco, G. García, S. J. Buckman, and M. J. Brunger, J. Chem. Phys. **132**, 074309 (2010).
[7]P. Limão-Vieira, M. Horie, H. Kato, M. Hoshino, F. Blanco, G. García, S. J. Buckman, and H. Tanaka, J. Chem. Phys. **135**, 234309 (2011).
[8]F. Blanco and G. García, Phys. Lett. A **360**, 707 (2007).
[9]F. Blanco, J. Rosado, A. Illana, and G. García, Phys. Lett. A **374**, 4420 (2010).
[10]H. Tanaka, T. Ishikawa, T. Masai, T. Sagara, L. Boesten, M. Takekawa, Y. Itikawa, and M. Kimura, Phys. Rev. A **57**, 1798 (1998).
[11]J. N. H. Brunt, G. C. King, and F. H. Read, J. Phys. B **10**, 1289 (1977).
[12]R. E. Kennerly, Phys. Rev. A **21**, 1876 (1980).
[13]S. K. Srivastava, A. Chutjian, and S. Trajmar, J. Chem. Phys. **63**, 2659 (1975).
[14]L. Boesten and H. Tanaka, At. Data Nucl. Data Tables **52**, 25 (1992).
[15]D. G. Thompson, J. Phys. B **4**, 468 (1971).
[16]D. Andrick and H. Bitsch, J. Phys. B **8**, 393 (1975).
[17]M. Bart, P. W. Harland, J. E. Hudson, and C. Vallance, Phys. Chem. Chem. Phys. **3**, 800 (2001).
[18]I. Sauers, L. G. Christophorou, and J. G. Carter, J. Chem. Phys. **71**, 3016 (1979).
[19]A. A. Christodoulides, L. G. Christophorou, R. Y. Pai, and C. M. Tung, J. Chem. Phys. **70**, 1156 (1979).
[20]S. Suzer, E. Illenberger, and H. Baumgärtel, Org. Mass Spectrom. **19**, 292 (1984).
[21]S. Feil, T. D. Märk, A. Mauracher, P. Scheier, and C. A. Mayhew, Int. J. Mass Spectrom. **277**, 41 (2008).
[22]F. Ferreira da Silva, D. Almeida, E. Vasekova, E. Drage, N. J. Mason, and P. Limão-Vieira, Chem. Phys. Lett. **550**, 62 (2012).
[23]M. Hoshino, M. Horie, H. Kato, F. Blanco, G. García, P. Limão-Vieira, J. P. Sullivan, M. J. Brunger, and H. Tanaka, J. Chem. Phys. **138**, 214305 (2013).
[24]H. Cho, R. J. Gulley, K. W. Trantham, L. J. Uhlmann, C. J. Dedman, and S. J. Buckman, J. Phys. B **33**, 3531 (2000).